Food and Chemical Toxicology 124 (2019) 411–422

Contents lists available at ScienceDirect

Food and Chemical Toxicology

journal homepage: www.elsevier.com/locate/foodchemtox

Flavonol glycosides in *Dyssodia tagetiflora* and its temporal variation, chemoprotective and ameliorating activities

E.A. Estrella-Parra[a], A.M. Espinosa-González[a], A.M. García-Bores[a], S.X. Zamora-Salas[a], J.C. Benítez-Flores[b], M.R. González-Valle[b], C.T. Hernández-Delgado[c], I. Peñalosa-Castro[a], J.G. Avila-Acevedo[a,*]

[a] Laboratorio de Fitoquímica, UBIPRO, FES-Iztacala, Unidad Nacional Autónoma de México, Av. de los Barrios No.1, Los Reyes Iztacala, Tlalnepantla, 54090, Estado de México, México

[b] Laboratorio de Histología, UMF, FES-Iztacala, Universidad Nacional Autónoma de México, Av. de los Barrios No.1, Los Reyes Iztacala, Tlalnepantla, 54090, Edo. de México, México

[c] Laboratorio de Farmacognosia, UBIPRO, Universidad Nacional Autónoma de México, Av. de los Barrios No.1, Los Reyes Iztacala, Tlalnepantla, 54090, Estado de México, México

ARTICLE INFO

Keywords:
Dyssodia tagetiflora
Flavonol glycosides
Temporary variation
UV radiation
Chemoprotective activity

ABSTRACT

Dyssodia tagetiflora is known as 'Tzaracata' and 'flor de muerto'. Recently, *D. tagetiflora* has been reported to have antioxidant activities in its polar extracts as well as insecticidal activities. Hyperoside (**1**), avicularin (**2**) and avicularin acetate (**3**) have been isolated previously. However, the temporary variation in glycoside flavonoids biosynthesis, as well as antibacterial and chemoprotective activities, have not been reported. The amount of **1**, **2** and **3** in the different collections was characterized by HPLC-MS. Two new C-glycosides were characterized, quercetin-4'-methyl ether 6-C glucoside (**A1**) and quercetin-4'-methyl ether 8-C glucoside (**A2**), as well as [2-(3,4-dihydroxyphenyl)-5,7-dihydroxy-4-oxochromen-3-yl]3,4,5-trihydroxyoxane-2,6-dicarboxylate (**A3**). This is the first report of the presence of C-C flavonoid glycosides compounds in the genus *Dyssodia*. Hyperoside was the majority compound at all collections. The methanolic extracts of August 2016 and October 2017 were active against *Micrococcus luteus* and *Bacillus subtillis*. The methanolic extract has chemoprotective effects because, when applied topically in SKH-1 mice, it decreases the severity of epidermal damage induced by acute exposure to ultraviolet radiation. In addition, cutaneous photocarcinogenesis was decreased in mice treated with the extract. The methanolic extract of *D. tagetiflora* has chemoprotective properties by decreasing the damage caused by acute and chronic exposure to UV in mice.

1. Introduction

The Tagetae tribe (family Asteraceae) comprises approximately 20 genera and 260 species concentrated in the most arid regions of America, especially abundant in México. Some representatives have been traditionally cultivated as plants of ornate and ceremonial use because of their striking flowers (Marotti et al., 2010). They are characterized by annual or perennial grass, with a shrub shape and alternate or opposite leaves, petiolate or sessile, with México as the main centre of diversification of this family (Villareal-Quintanilla et al., 2008). Thus, *Dyssodia tagetiflora* Lag., receives common names such as 'colado', 'Tzaracata' (Purépecha language) and 'flor de muerto'. This plant has been found in corn crops with saline soils on the shores. It is an arvense and ruderal plant, common in disturbed and open sites, especially in regions derived from the low deciduous forest mesophilic and oak forests. The plant emerges in May and begins to flower in September and concludes its flowering in November; later, it has a latent life as a rhizome (Sánchez-Blanco and Guevara-Féfer, 2013).

Few chemical studies have been performed on the genus *Dyssodia*. *D. anthemidifolia* has been reported to contain the compound 5-methyl-2,2':5',2"-terthiophene (Downum et al., 1985), and bithhiennyl and terthienyl compounds are found in *D. decipienns* (Bolhmann and Zdero, 1979; Downum and Towers, 1983), *D. papposa* (Downum and Towers, 1983) and *D. acerosa* (Bolhmann and Zdero, 1976). Meanwhile, *D. acerosa* has been reported to comprise an essential oil that contains a high proportion of monoterpenes such as chrysanthenone and camphor,

* Corresponding author. Laboratorio de Fitoquímica, UBIPRO, FES-Iztacala, Universidad Nacional Autónoma de México, Av. de los Barrios No.1, Los Reyes Iztacala, Tlalnepantla, 54090, Estado de México, México.
E-mail address: tuncomaclovio2000@yahoo.com.mx (J.G. Avila-Acevedo).

https://doi.org/10.1016/j.fct.2018.12.024
Received 7 September 2018; Received in revised form 12 December 2018; Accepted 17 December 2018
Available online 18 December 2018
0278-6915/

among other compounds (Tellez et al., 1997). Moreover, in medicinal folklore, the Otomi people from México used *D. pinnata* to treat gastrointestinal disorders (Rojas et al., 1999). Recently, in *D. tagetiflora*, the insecticidal activity of the essential oil against *D. melanogaster* (LD_{50} = 30.9 μg/mL) was reported. The methanolic extract showed antioxidant activity (IC_{50} = 19 and 4.8 μg/mL; DPPH and ABTS, respectively). Additionally, quercetin glycosides: hyperoside, avicularin, and acetyl-avicularin were isolated from the methanolic extract (García-Bores et al., 2018). Quercetin is commonly found in its glycoside form, in which one or more hydroxyl groups is replaced by different sugar groups. Many plants and vegetables contain quercetin O-glycosides, and the most common glycosylation site is located at the C-3 carbon (Geng et al., 2016). Although C-glycosides are another type of quercetin derivative, these compounds occur rarely in nature (Materska, 2008). Additionally, it was reported that phenolic compounds in birch leaves (*Betula pubescens*) are decreased during the growing season (Nurmi et al., 1996), but the contents of secondary metabolites can be associated with UVB radiation and low temperature, which are prevalent at high altitudes (Cirak et al., 2017).

Our group aimed to study Mexican flora in the search of secondary metabolites with chemoprotective properties. The objective of the present study was to determine the temporal variation of flavonol glycosides and to determine the antibacterial activity and chemoprotective capacity of the methanolic extract of *D. tagetiflora* (MEDt) against the damage caused by acute and chronic exposure to ultraviolet radiation (UVB) in a murine model.

2. Material and methods

2.1. Plant material

The aerial parts of *D. tagetiflora* were collected in August 2016, August 2017, September 2017 and October 2017 on 'Cerro del Toro' in the Province of Acámbaro (Guanajuato, México) at 20°01'67'' north latitude, 100°7′ west longitude and 2000 m above sea level (m.a.s.l.). In addition, *D. tagetiflora* was collected only in October 2017 on the 'Los Agustinos' reserve, located at 20°12'51rsquo;' north latitude, 100°39'19'' west longitude at 2750 m.a.s.l., Acámbaro, (Guanajuato, México). The plant was authenticated by M. en C. Edith López Villafranco and was deposited in the IZTA Herbarium of the Facultad de Estudios Superiores-Iztacala, Universidad Nacional Autónoma de México, where a voucher specimen was registered as No. 20417 IZTA.

2.2. Extraction of D. tagetiflora

The aerial parts of all collections were dried to ambient temperature, in a room without natural light. Posteriorly, the plants (13.50 g) were pulverized and powdered. The powder was extracted by maceration successively with hexane, dichloromethane and finally with methanol at a ratio of 1:10 (w/w). Three consecutive macerations with each solvent were performed at 25 °C. Each extract was filtered and concentrated under reduced pressure. The yield of methanolic extract (MEDt) obtained at each collected season was calculated based on the ratio of the solids obtained and mass of the plant material used for extraction. On average, 1.50 ± 0.25 g of MEDt was obtained at a yield of approximately 11.11% each. MEDt obtained in August 2017 was used for experiments of biological activity.

2.3. Phytochemical composition and temporal variation of MEDt

2.3.1. HPLC/DAD

The HPLC apparatus consisted of a diode array with UV-ESI-MS detection. Chromeleon Software was used. The system consisted of a PDA detector (at 254–350 nm). The column was an Allsphere ODS-1 (150 mm × 4.6 mm, 5 μm). The samples were analysed using a linear gradient of 0.1% formic acid in water (v/v) (A), 0.1% formic acid in acetonitrile (v/v) (B) and 0.1% acid formic in methanol (v/v) (C): starting with 95% A, 2% B and 3% C, and ending at 20 min with 43% B and 57% C. The flow rate was 1.2 mL/min, and a quaternary 600 pump was connected to an autosampler cooled to 20 °C. The following compounds were used for quantification: hyperoside, avicularin, and avicularin acetate. These compounds were previously isolated and characterized by NMR (García-Bores et al., 2018). Quercetin was purchased from Sigma-Aldrich (Q0125-10).

2.3.2. Mass detector

2.3.2.1. Full mass. An Orbitrap Fusion Tri-hybrid system was used with an ESI source controlled by Xcalibur Software (Thermo Scientific Xcalibur V. 4.1.5.0). The operating parameters were as follows: ion transfer tube temperature (°C): 260; vaporizer temp (°C): 350; detector type: ion trap; use quadrupole isolation: true; scan range (*m/z*): 50–1000; polarity: positive; intensity threshold: 5.0e4; mass range (*m/z*): 50–1000; isolation mode: quadrupole; HCD collision energy (%): 35; first mass (*m/z*): 50; AGC target: 5.0e4. Nitrogen and helium of ultra-high purity were used as nebulizing gases.

2.3.2.2. $ddMS^2$ OT HCD. The operating parameters were as follows: MS^n level: 2; isolation mode: ion trap; use isolation *m/z* offset: false; activation type: HCD; HCD collision energy (%): 50; detector type: Orbitrap; scan range mode: auto, *m/z* normal; Orbitrap resolution: 60000; first mass (*m/z*): 50; AGC Target: 1.5e5; inject ions for all available parallelizable time: false; maximum injection time (ms): 35; microscans: 1; data type: centroid; use EASY-IC: false.

2.3.2.3. $ddMS^3$ OT HCD. The operating parameters were as follows: MS^n Level: 3; synchronous precursor selection: false; use isolation *m/z* offset: false; activation type: HCD; HCD collision energy (%): 50; detector type: Orbitrap; scan range mode: auto, *m/z* normal; Orbitrap resolution: 60000; first mass (*m/z*): 50; AGC target: 1.5e5; inject ions for all available parallelizable time: false; maximum injection time (ms): 35; microscans: 1; data type: centroid; use EASY-IC: false.

2.4. Antibacterial activity of MEDt and isolated compounds

2.4.1. Qualitative assay: Kirby Bauer (disk-diffusion method)

The antibacterial activity was evaluated by the disk-diffusion method (Marín-Loaiza et al., 2008). A disk of 5 mm diameter of Whatman paper number five was prepared; each of them was impregnated with methanolic solutions of each extract or isolated compounds until the amount reached 2 mg per disk, followed by incubation overnight to evaporate. *Serratia marcescens* (ATCC14756) (Gram -), *Bacillus subtilis* (168WT) (Gram +) and *Micrococcus luteus* (ATCC10240) (Gram +) were used due to ecologic importance. Microorganisms were grown overnight at 37 °C in 10 mL of Mueller–Hinton broth. The cultures were adjusted with sterile saline solution to obtain turbidity comparable to that of McFarland No. 0.5 standard (1.0×10^8 CFU/mL). Petri dishes containing Mueller–Hinton agar were inoculated with these microbial suspensions. MEDt and pure compounds with impregnated disks were placed in Petri dishes containing the test microorganisms. Disks with chloramphenicol (30 μg) were used as positive controls. After 24 h of incubation, inhibition halos were measured. Each experiment was repeated three times.

2.4.2. Quantitative assay

The broth dilution method was used to determine the concentrations at which the substances inhibit the growth of microorganisms (modified from Koneman et al., 2017). The technique is based on the use of 2,3,5-triphenyl tetrazolium chloride (TTC), a salt that is pale yellow and, when reduced enzymatically to 1,3,5-triphenylformazan or formazan, changes to red when the cells are alive, due to the activity of several dehydrogenases. The assay using this technique is fast, efficient and reliable to quantify cell viability colourimetrically.

The substances tested were those that demonstrated antimicrobial activity in the Kirby Bauer qualitative test: MEDt, avicularin acetate and avicularin-avicularin acetate (1:4). The concentrations used for each compound were: 0, 0.125, 0.25, 0.5, 0.75, 1.0, 1.5 and 2 mg/mL.

The experiment was carried out in 96-well plates, where 50 μL of bacterial suspension was inoculated at a final concentration of 1×10^5 bacteria/mL in each well. Subsequently, the different concentrations of the substances were placed in the corresponding well. The plate was incubated at 37 °C for 24 h. Thereafter, 50 μL of TTC was incorporated to 0.08% (w/v) and incubated during 30 min at 37 °C for later reading.

The results were interpreted from the formation of formazan crystals and the red coloration they produce. The concentration at which the coloration is no longer observed is considered the minimum inhibitory concentration (MIC), and the next concentration is the minimum bactericidal concentration (MBC).

2.5. Chemoprotective assays

2.5.1. Experimental animals

The SKH-1 hairless mouse strain, a widely used model for human photocarcinogenesis, was used in our study. Female SKH-1 mice at 5–6 weeks of age (weighing 27 ± 5 g) were purchased from Charles River Laboratories (Wilmington, MA) and were maintained in a climate-controlled environment with a 12 h light/dark cycle. Five mice were used per cage and were acclimatized for two weeks before starting the experiment. Throughout the experimental period, mice had free access to food and water that were provided through the food chamber on top of the cages. The Bioethical Committee/FES Iztacala, UNAM approved all animal protocols.

2.5.2. In vivo MEDt penetration study: tape stripping

Female SKH-1 mice at 5–6 weeks of age (n = 5, weight on 27 ± 5 g) were placed in a laminar flux chamber at 21 °C and 62% relative humidity for 30 min. Application zones measuring $2 \times 2\ cm^2$ was marked for each mouse in the dorsal area. The MEDt was applied to the surface of the skin at 4 mg/cm^2. Fifteen minutes after an application, the excessive substance on the applied area was wiped off with a cotton swab, followed by washing with 96% ethanol and drying. The stratum corneum of the treated areas was removed by four successive tape strippings using Scotch tape strips (19 mm × 32.9 m; 3 M, MN, USA). Each strip was taken in a controlled way, i.e., a 10 g rubber weight was rolled over it 10 times. The first strip was discarded, and the three following strips were collected and deposited in a 20 mL beaker. Five mL of ethanol were added at each sample and then were stirred with a magnetic bar for 30 min. The absorbance was measured at 365 nm using a double-beam spectrophotometer (Perkin-Elmer, Lambda 2S UV/VIS) because the MEDt main components absorbed that wavelength. MEDt penetration was obtained in accordance with the concentration measurements calculated by regression analysis (Lademann et al., 2009; Wissing and Müller, 2002).

2.5.3. Protocol for acute and chronic experiments of chemoprotection

The SKH-1 mice were randomly divided into four groups of five mice each: negative control (C-), positive control with UV (C + UV), MEDt and MEDt irradiated with UV (MEDt UV). The mice in the negative and positive control groups were treated topically on the dorsal skin with 200 μL of 70% ethanol (exposed area: 4 cm^2). MEDt was dissolved in 70% ethanol at a concentration of 40 mg/mL (Espinosa-González et al., 2016). The MEDt groups were treated topically on the dorsal skin with 8 mg/200 μL of the respective test solutions.

Fifteen minutes after application of the substances, the C + UV and MEDt UV groups were irradiated with UVB lamps (302 nm, UVP. UVM-26, 6 W) positioned 15 cm above their backs. Irradiation at this distance produced a dose of 6 mJ/cm^2, which was measured using a Spectroline model DM-300HA research radiometer. The irradiation exposure time in acute experiments was 10 min. After 24 h of irradiation, erythema was measured. Animals were subsequently sacrificed by carbon dioxide asphyxiation, and the dorsal skin was dissected (Avila Acevedo et al., 2014).

To study chemoprotection at a chronic level, it was preceded in the same way as the acute study, regarding the number and characteristics of the mice, and the classification of the lots (C-, C + UV, EMDt, EMDt UV). The irradiation protocol was the same, only the time and chronicity of the irradiation were different. In this case, the irradiation consisted of exposure to UVB for 1 min each day for ten days. Subsequently, the mice were irradiated three times a week for 1 min for 33 weeks, which is congruent with the treatments and time for the previous occurrence of tumours in these mice (Gallagher et al., 1984). The time of appearance of tumours was mapped for each mouse. Skin tumour formation, indicated by the presence of outgrowths with a diameter of 1 mm or greater, was expressed as the tumour incidence and average tumour multiplicity (average number of tumours per mouse) for each irradiated group (Wang et al., 1992) To evaluate the incidence and multiplicity of lesions, a count was performed weekly to determine the number of injuries.

2.5.4. Erythema measurements

The erythema in mice in acute experiments was calculated by measuring the skin redness of the dorsal area of mice using a colour analyser (Lutron, Mod. RGB-1002). Among the various methods, colourimetry has the advantage of being the simplest and most reproducible method. Redness values were measured 24 h after irradiation. The results are expressed as redness values for each treatment (Trujillo et al., 1996).

2.5.5. Histological observation of the skin in acute experiments

Each dorsal skin sample was fixed with 2% paraformaldehyde in phosphate buffer solution (pH 7.2) for 24 h in the tissue embedding cassette, dehydrated with a sequence of ethanol solutions (70%, 80%, 95% and 100% v/v) and embedded in paraffin. All serial sections were cut to a thickness of 5 μm, de-paraffinized, and stained with haematoxylin-eosin (H&E) and toluidine blue to identify and quantitate mast cells. The histopathological changes of each section were observed using multiple microscopic fields and were photographed using a photomicroscope (Leica DM500). The histological diagnosis was performed comparing the C- mouse skin samples with the UVB-irradiated groups (Elder et al., 1997). The classification of histological damage caused by UVB was carried out in the presence or absence of damage in the epidermis and dermis. The grade (mild, moderate or severe) and the extension of the lesions in the observed fields (focal, multifocal or diffuse) (Lashmar et al., 1988). Each value of the extension and grade was assigned a number (1, 2 and 3) (Robbins et al., 2008; Sharma et al., 2011).

2.6. Statistical analysis

Statistical analysis was performed on the collected data. The mean values of the negative and positive controls and MEDt groups were obtained from descriptive analyses, and one-way ANOVA was conducted to obtain F values and MS errors. Dunnett's test was used to determine the level of significance compared with the negative and positive control values in each experimental series.

3. Results and discussion

3.1. Phytochemical composition and temporal variation of MEDt

We identified six compounds in the methanolic extracts. Among them, hyperoside (**1**), avicularin (**2**), and avicularin acetate (**3**) were isolated and reported previously (García-Bores et al., 2018). In this work, three other compounds were identified by LC-ESI-MS: quercetin-4'-methyl ether 6-C glycoside (**A1**) [M + H 481.00 *m/z*], quercetin-4'-

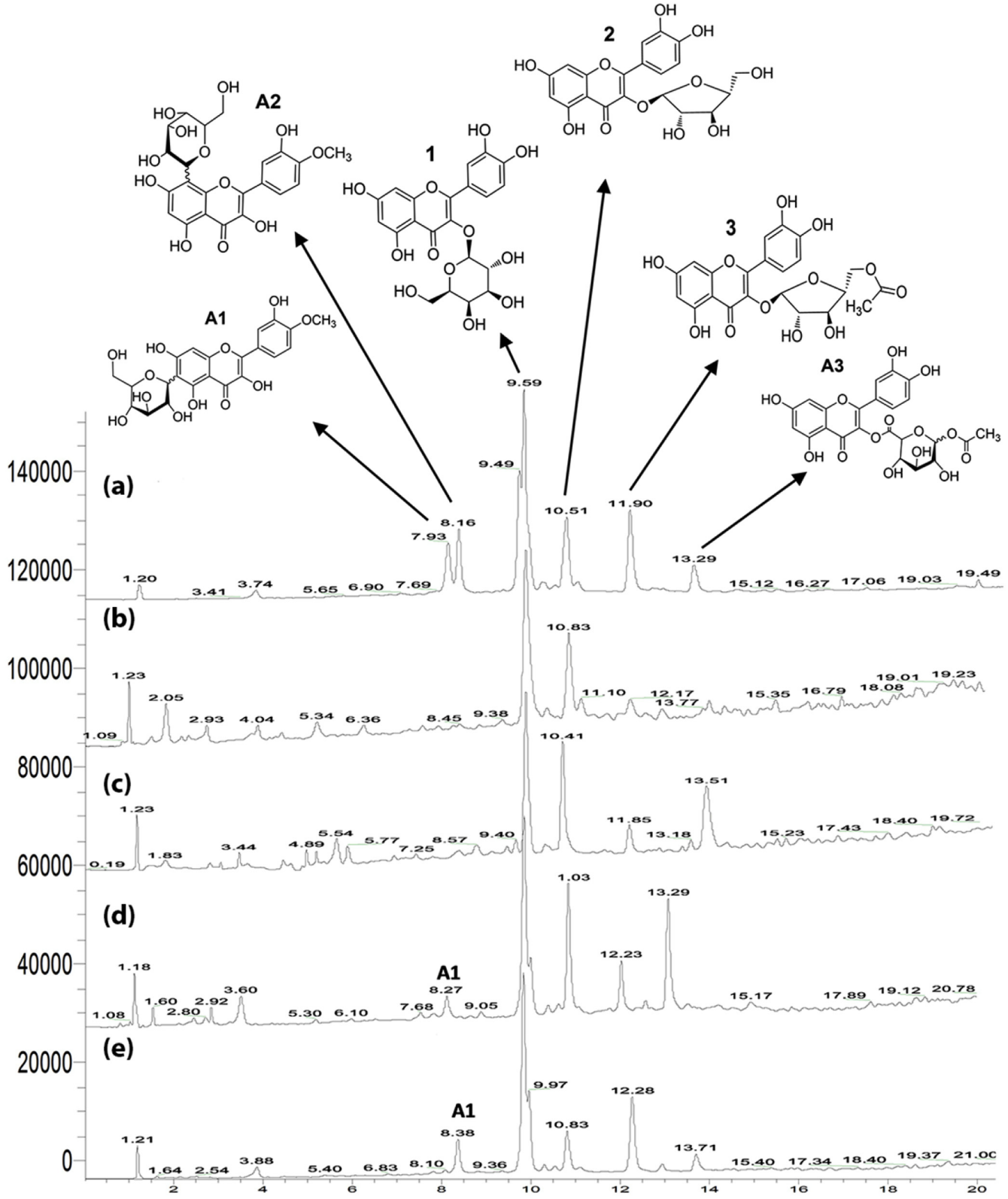

Fig. 1. Chromatogram of the methanol extracts of *D. tagetiflora*: (a) August 2016, (b) August 2017, (c) September 2017, (d) October 2017 (locality 'Cerro el Toro'), (e) October 2017 (locality 'Los Agustinos'). Compounds: **A1**. quercetin-4'-methyl ether 6-C glycoside; **A2**. quercetin-4'-methyl ether 8-C glycoside; **A3**. [2-(3,4-dihydroxyphenyl)-5,7-dihydroxy-4-oxochromen-3-yl] 3,4,5-trihydroxyoxane-2,6-dicarboxylate; **1**. hyperoside; **2**. avicularin; **3**. avicularin acetate.

methyl ether 8-C glycoside (**A2)** [M + H 481.10 *m/z*] and [2-(3,4-dihydroxyphenyl)-5,7-dihydroxy-4-oxochromen-3-yl]3,4,5-trihydroxyoxane-2,6-dicarboxylate (**A3**) [M + H 521.07 *m/z*]. Additionally, in samples collected in October 2017 in both localities ('Cerro del Toro' and 'Los Agustinos'), we identified compound **A1** (Fig. 1).

From the compounds isolated and reported previously (García-Bores et al., 2018), hyperoside was present at all collection dates and was the majority compound (0.036–0.18 mg/mg of extract). Furthermore,

Table 1
Quantification of the compounds present in the four different collects.

Compound	Date of collect (mg of compound/mg of extract)				
	August 2016	August 2017	September 2017	October 2017	October 2017[a]
Hyperoside	0.189 ± 0.06	0.033 ± 0.0006	0.036 ± 0.001	0.056 ± 0.003	0.09 ± 0.009
Avicularin	0.047 ± 0.008	0.009 ± 0.0001	0.015 ± 0.0005	0.020 ± 0.0003	0.0159 ± 0.003
Avicularin acetate	0.107 ± 0.04	0.006 ± 0.0007	0.012 ± 0.002	0.016 ± 0.001	0.049 ± 0.02

[a] Collected at 'Los Agustinos. (Mean ± SD, n = 3).

avicularin and avicularin-acetate were the second and third majority compounds, in September and October 2017, respectively ('Cerro del Toro', Acámbaro, Gto, México) (Table 1).

3.2. Analysis of *A1* and *A2* compounds

3.2.1. Analytes with retention time of 7.9 and 8.1 min

We proposed that the analytes with retention time of 7.9 and 8.1 min present in August 2016 samples were quercetin-4'-methyl ether 6-C glycoside (**A1**) [M + H 481.00 *m/z*] and quercetin-4'-methyl ether 8-C glycoside (**A2**) [M + H 481.10 *m/z*]. Likewise, the analyte present in October 2017 samples at both locations ('Cerro del Toro' and 'Los Agustinos') corresponded only to **A1** (Fig. 1). To our knowledge, this is the first time both compounds have been reported in *D. tagetiflora*.

3.2.2. Mass spectra analysis of *A1* and *A2* aglycone

In the August 2016 sample containing **A1** and **A2** (RT: 7.9 and 8.1 min, respectively), as well as in October the 2017 sample containing (**A1**) ('Cerro del Toro' and 'Los Agustinos' locations) (RT 8.2 and 8.3 min, respectively), we found 4'-methyl ether quercetin [M + H 317 *m/z*; 8% intensity] to be the aglycone of **A1** and **A2**.

It has been widely reported that the retro-Diels-Alder (RDA) reaction is a common feature that provides information on the number and type of substituents in the A and B rings in flavonoids (Cuyckens and Claeys, 2004). Therefore, the RDA reaction in the A ring generated the fragment ions 311 *m/z* (glycosylated; 8% intensity), 153 *m/z* (without sugar; 10% intensity) and 126 *m/z* (10% intensity). Additionally, the RDA reaction in the B ring generated the fragment ions 167 and 138 *m/z* (10% intensity). Those ion fragments are of interest here because they provide information about the methoxy group, which is present in the C-4′ in the B ring. Additionally, the absence of the ion fragments 137, 108, and 91 *m/z* (Fig. 2 crossed arrow) denote a non-existent pathway. This showed that the methoxy group is present in the B ring, and not in another place of the aglycone. Finally, the mass fragmentation of quercetin was compared with our experimental mass spectra, being different for 15 *m/z*. In conclusion, the aglycone identified is the compound quercetin-4'-methyl ether commonly called 'tamarixetin' (D'Andrea, 2015) (Fig. 2).

3.2.3. Mass spectral analysis of *A1* and *A2* glycosides

The mass spectra obtained showed two different fragmentation patterns of the O- and C- glycosides. For example, hyperoside, which is an O-C glycoside, showed a base peak at 303 *m/z*, indicating that the binding between the aglycone and sugar is labile and corresponds to a glycosidic bond (Abad-García et al., 2008, 2009; Geng et al., 2016) (Fig. 3b). By contrast, 4'-methoxy quercetin 6-C and 8-C glycoside (**A1** and **A2**, respectively) showed a poor peak [M + H 317 *m/z*; 6% intensity] that is consistent with the C-C link between the flavonoid and glycoside (Fig. 3c and d); thus, the flavonoid C-glycosides are more stable than aglycones or O-glycosides (Xiao et al., 2016). The flavonoid C-glycosides usually need higher collision energies, which induce the primary breaks that occur in the sugar ring (Abad-García et al., 2008, 2009, Geng et al., 2016). This phenomenon is evident by the appearance of ion fragments corresponding to the loss of water molecules at 120 and 90 *m/z* (Fig. 4a) (Sánchez-Rabaneda et al., 2003; Cuyckens and Claeys, 2004).

3.2.4. Difference between the 6-C (*A1*) and 8-C (*A2*) glycosides

As mentioned previously, the main feature of the C-glycosidic bond, is that the sugar is directly linked to the flavonoid nucleus via an acid-resistant C-C bond (Cuyckens and Claeys, 2004; Abad-García et al., 2009). Stability of the C-glycosidic bond needs high collision energies for its fragmentation (De Villiers, 2016). In this point, the goal was the differentiation between the 6-C and 8-C glycoside flavonol.

In our experiments, the loss of water and COH_2 is present in both spectra. However, in the 6-C glycoside, the intensity of those fragments is higher than that in the same fragments of the 8-C glycoside (Table 2). This dehydration is one feature of the fragmentation pathway of the sugar ring. Waridel et al. (2001) reported that the loss of water was more intense in isoorientin (6-C glycoside) than in orientin (8-C glycoside). Additionally, in our experiments, we note the presence of an ion fragment at 463 *m/z* [M + H-18 *m/z*], which is due to the loss of one molecule of water, being more intense in the 6-C glycoside (2%) than in the 8-C glycoside (< 1%) (Table 2; Fig. 4a and b).

Additionally, we can observe the ion 409 *m/z* [M + H −4 H_2O], which, in the 8-C glycoside, was less intense (3%) than that in the 6-C glycoside (4%) (Table 2; Fig. 3c and d). This indicates that the 6-C glycoside can eliminate -via the loss of water- the hydroxyl group present in C-5 and C-7 of tamarixetin (Fig. 4b). In contrast to the 8-C glycoside, the loss of water is only in the C-7 to tamarixetin, reducing the intensity of the loss of water signal in the spectra (Table 2; Fig. 4b). This is in accordance with previously reported results by Abad García et al. (2009), who reported that luteolin and apigenin 6-C glycoside presented the loss of four water molecules [M + H-72 *m/z*], in contrast to luteolin and apigenin 8-C glycosides and did not present these losses. Additionally, it was reported that, in 8-C glycosides, the fragment [M + H −4 H_2O] was low in intensity; however, in 6-C, it was more perceptible. Similar results of 6-C and 8-C flavonoids glycosides were reported by Geng et al. (2016).

Moreover, in our experiments, the ion 331 *m/z* (M + H-150 *m/z*) in the 6-C glycoside presented low intensity (2%), while that in the 8-C glycoside was higher (4%). Thus, Pereira et al. (2005) reported that the loss of 150 *m/z* in isoorientin (6-C glycoside) was less intense (40%) than that in orientin (8-C glycoside) (60%).

Otherwise, we can observe the ions of 361 *m/z* [M + H −120 *m/z*] that, in both spectra, present similar intensity (3%) (Table 2). This is in partial disagreement with the results previously reported by Grayer et al. (2000), who mentioned that C-glycosides in *Ocimum gratissimum* presented the loss of [M + H −120 *m/z*], which, in 8-C glycosides, were the most intense than 6-C glycosides. Additionally, Pereira et al. (2005) reported particularly that the loss of [M + H −120 *m/z*] in isoorientin (6-C glycoside) was less intense than that in orientin (8-C glycoside). Finally, Singh et al. (2015) reported that, in the loss of 90 *m/z* in luteolin and apigenin 6-C glycoside, the ion fragment was more abundant than in the 8-C glycoside. The pattern of fragmentation shown in Table 2 and Fig. 4a indicates that the sugar suffers the loss of four water molecules, suggesting that the sugar bound to the flavonoid is a glucose, due to similar pattern of fragmentation obtained experimentally with the reported by Abad García et al. (2009). At this time, it was not known between the two C-glycosides (**A1** and **A2**) which had

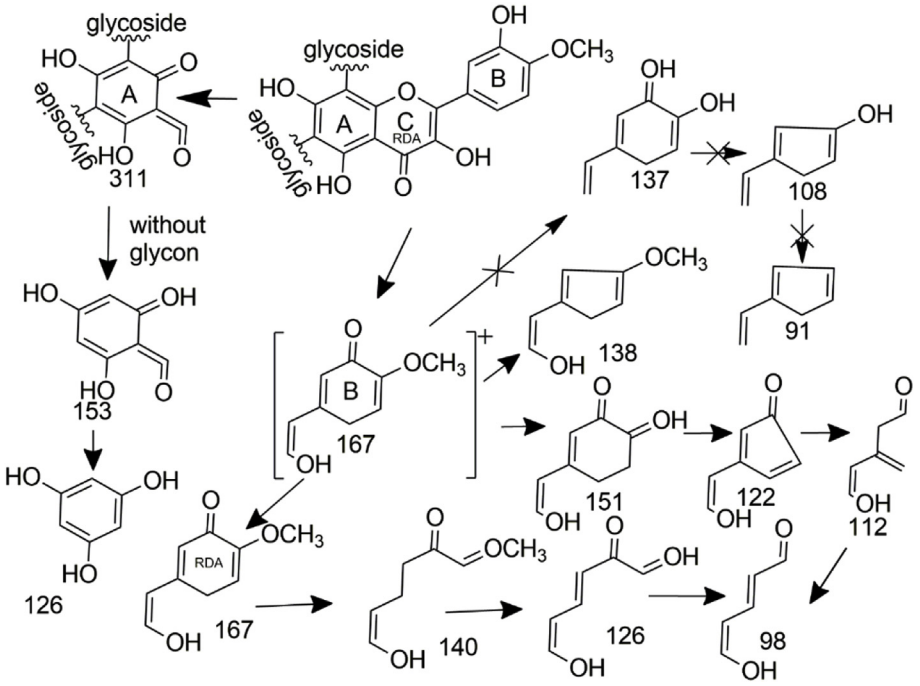

Fig. 2. Fragmentation of the quercetin-4′-methyl ether (tamarixetin).

the C-6 or C-8 bond. Therefore, to assign the ion fragments (361, 391 and 409 *m/z*) in each molecule, it was decided to carry out MS/MS experiments (MS^2 and MS^3).

To distinguish between 6-C (**A1**) and 8-C (**A2**) glycosides, both analytes were evaluated via MS^2 and MS^3, using HCD collision energy at 50%. Thus, we can find an evident difference in both analytes. The ion fragments 391 [M + H-90 *m/z*; 90% intensity] and 409 [M + H-72 *m/z*; 10% intensity] were only present in the 6-C (**A1**) glycoside. Meanwhile, the ion 361 [M + H-120 *m/z*; 100% intensity] was only present in the 8-C (**A2**) glycoside. This agrees with the results previously reported by Harborne (1994); Ferreres et al. (2003); Sánchez-Rabaneda et al. (2003); Pikulski and Brodbelt (2003); Davis and Brodbelt (2004) and Cao et al. (2014).

Finally, it was not possible to isolated preparatively **A1** and **A2** from MEDt due to its low yield. In the future studies, will isolated them to confirm structures via NMR (^1H and ^{13}C), especially the realization of NOE correlation experiment to assign the type of bond (α or β) between sugar and aglycone.

3.3. Mass spectral analysis of *A3*

We proposed the compound [2-(3,4-dihydroxyphenyl)-5,7-dihydroxy-4-oxochromen-3-yl]3,4,5-trihydroxyoxane-2,6-dicarboxylate [M + H 521.07 *m/z*) as the last analyte in the chromatogram (RT 13.29 min) (Fig. 1; **A3**) that is present in all seasons of collection. For practical purposes, the sugar was placed in the 3-C position; however, the sugar can be located in other OH substituents. Thus, the exact mass *in silico* [520.09 *m/z*] (ChemBiodraw Ultra, V. 12.0) is similar in our experiment [M + H 521.07 *m/z*] (Fig. 5). Therefore, the fragmentation pattern presents a peak at 303 *m/z* [M+H] corresponding to quercetin. Moreover, the loss of COH_2 generated a high intensity of ion 333 *m/z* [M+H]. Furthermore, the sugar part presented the loss of three water molecules, indicating the presence of OH groups. Among other features, the dissociation of the sugar part induces an acylium ion (HCO^+) and carbenium ions ($C_2H_4^+$, CH_3^+). Fig. 5 shows the sugar dehydration pattern. Likewise, in other fragments, the α-cleavage to the carbonyl group is evident, inducing an acyl ion loss [M + H −43 *m/z*]. The mass spectrum obtained in this study is similar to that obtained by Simkhada et al. (2010) for O-glucuronyl quercetin. In conclusion, the compound **A3** is [2-(3,4-dihydroxyphenyl)-5,7-dihydroxy-4-oxochromen-3-yl] 3,4,5-trihydroxyoxane-2,6-dicarboxylate.

3.4. Antimicrobial activity of MEDt and isolated compounds

It was reported that quercetin glycosides are produced by some plant species as an eliciting response against microorganisms (Conceição et al., 2006). Thus, we proceeded to evaluate the antibacterial activity against three common bacteria in the environment, that can contaminate foods. As mentioned previously, hyperoside and avicularin were the first and second majority compounds in almost all samples of MEDt. Nevertheless, it showed no inhibition against tested bacteria. By contrast, the MEDt of the August 2016 ('Cerro del Toro') sample and October 2017 (Collected at 'Los Agustinos') sample presented an antibacterial effect against *M. luteus* as well as *B. subtillis*, being inactive against *S. marcescens*. Here, it is important to note that only the active extracts have in their chemical composition C-C glycosides and O-glycosides. Meanwhile, avicularin acetate and the mixture of avicularin/avicularin acetate (1:4) presented activity only against *M. luteus* (Table 3). This fact agrees with that found by Wu et al. (2013), who demonstrated a positive correlation between the deleterious effect and hydrophobicity of the flavonoids with respect to their activity on the membranes of Gram-negative bacteria. Thus, the MEDt containing mainly quercetin glycosides demonstrated no activity on *S. marcescens*. Accordingly, it is presumable that MEDt is only active against Gram-positive bacteria.

There are few reports on the activity of C-flavonoid glycosides. The antimicrobial activity of the shamimin has been reported as a 6-C flavonol glycoside that was isolated from *Bombax ceiba* and that has structural similarity to **A1** (Faizi and Ali, 1999). It is likely that the antibacterial activity of the extracts collected in August 2016 ('Cerro del Toro') and October 2017 ('Los Agustinos') is due to the synergy between avicularin acetate and **A1** because these two collections were detected in larger quantities (Fig. 1).

To confirm the bactericidal activity of extracts and compounds, we obtained the minimal concentration inhibitory (MIC) and minimum bactericidal concentration (MBC). For this purpose, we tested the

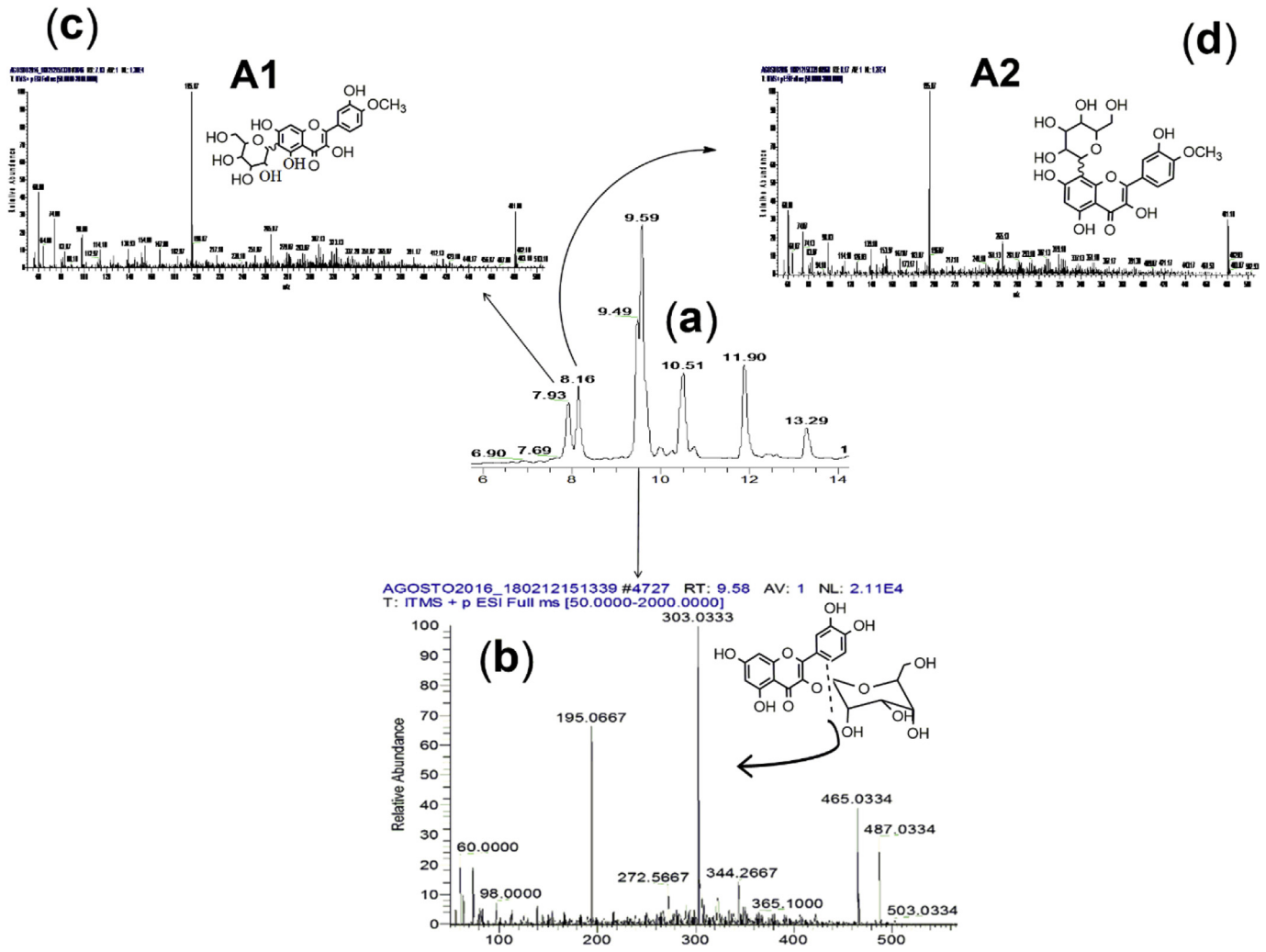

Fig. 3. Full mass and chromatogram of the **A1** and **A2** analytes. (a) Chromatogram of August 2016 sample. (b) Full mass of hyperoside, which can observe the high intensity of the bond between quercetin and glycoside part [303 *m/z*; 100% intensity]. (c) Full mass of quercetin-4'-methyl ether 6-C (**A1**). (d) Full mass of quercetin-4'-methyl ether 8-C (**A2**).

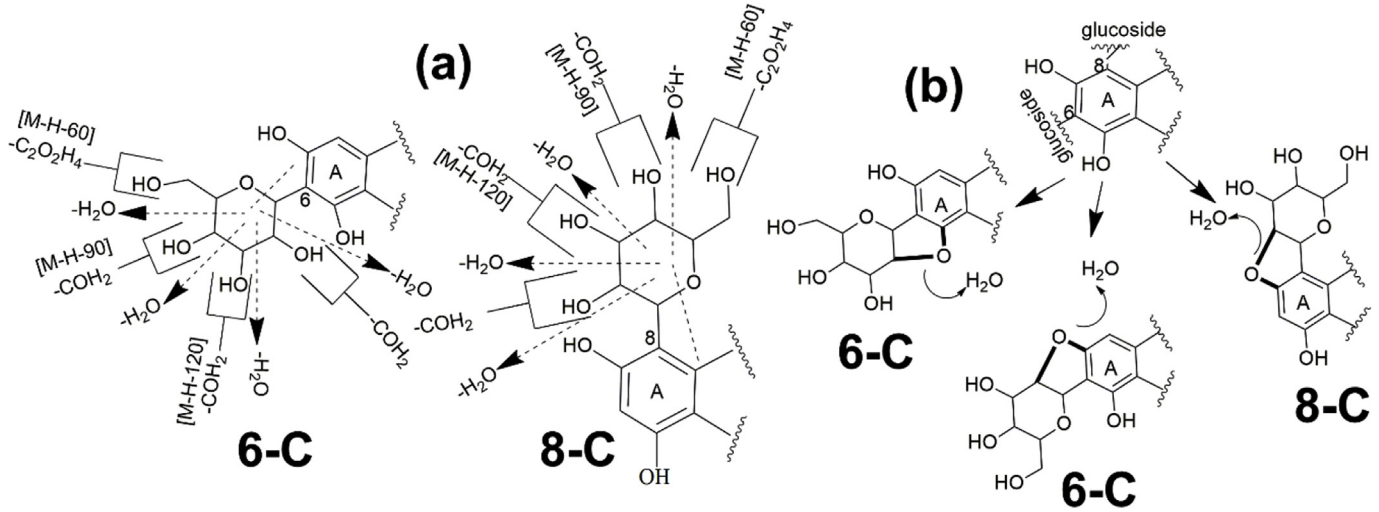

Fig. 4. Loss of water and COH_2 in 6-C (**A1**) and 8-C (**A2**) glycosides. (a) Loss of water (18 *m/z*) and COH_2 (30 *m/z*) in 6-C and 8-C. (b) Interaction of the hydroxyl group in C-5 and C-7 position in the A ring of the aglycone, with the hydroxyl group to sugar.

Table 2
Loss of water in 6-C and 8-C glycosides (Full mass).

Ion	Loss	Position of the glycone part			
		6-C (A1)		8-C (A2)	
		(RT: 7.93 min) *m/z*	Intensity (%)	(RT: 8.17 min) *m/z*	Intensity (%)
M + H	0	481.0	32	481.1	28
-H_2O	18	463.0	2	463.0	< 1
−2 (H_2O)	36	445.0	< 1	445.0	< 1
−3 (H_2O)	48	427.0	2	427.0	< 1
$C_2O_2H_4$	60	421.0	< 1	421.1	4
−4 (H_2O)	72	409.0	4	409.0	3
$C_3O_3H_6$	90	391.1	6	391.3	3
$C_4O_4H_8$	120	361.0	3	361.0	3
$C_5O_5H_{10}$	150	331.0	2	331.0	4

extract October 2017 ('Los Agustinos') as well as the compounds avicularin acetate and avicularin/avicularin acetate (1:4). The extract collected in October 2017 ('Los Agustinos') presented a lower MIC and MBC than the isolated compounds, indicating a probable synergy between **A1** and the acetate of avicularin (Table 4).

3.5. Chemoprotective assays

3.5.1. MEDt penetration study

The results of HPLC-MS analysis of the MEDt confirmed the presence of hyperoside, avicularin and avicularin acetate. Because all three compounds have maximum absorption peaks (λmax) near 365 nm, this wavelength was chosen for their detection in the permeation experiments. Similar to the irradiation experimental protocol, each mouse was treated topically with 4 mg/cm^2 of the MEDt for 15 min. Active components of MEDt penetrate at 0.43 ± 0.2% (18 μg/cm^2). The quercetin glycosides are the main components of MEDt that have been reported to have different biological properties, including antioxidant, cytoprotective (García-Bores et al., 2018) and anti-inflammatory capacities (Sharma et al., 2018). However, quercetin has poor solubility. This flavonoid has a partition coefficient of 1.82 ± 0.32 due to the presence of non-polar groups, but hydroxyl in carbons 3 (ring C), 5 and 7 (ring A) as well as in carbons 3′ and 4' (ring B) decrease its ability to penetrate the skin (Hatahet et al., 2016). Avicularin and hyperoside are glycosides that increase their polarity; therefore, their penetration of the skin is poor. This would lead to the notion that the quantity of active compounds of MEDt that penetrates the skin is low; however, the number of molecules that can penetrate is significant according to Avogadro's number (Avila Acevedo et al., 2014) and can have effects on the skin.

3.5.2. Chemoprotection in acute experiments

3.5.2.1. MEDt anti-erythema activity. One of the principal events in acute skin UVB irradiation exposure is the production of erythema (skin redness). Erythema is visible 24 h after exposure to UVB. As shown in Fig. 6, irradiated unprotected SKH-1 mice exhibited increased skin redness within 24 h of UV exposure. Both groups of mice treated with MEDt (MEDt and MEDt UV) showed a decrease in redness compared with the unprotected irradiated group ($p < 0.05$).

Regarding erythema, the determining factor of skin colour is the extent to which vascular filling occurs, where an increase or decrease in vessel congestion results in a greater degree of redness or paleness of the skin, respectively (Trujillo et al., 1996). Exposure of the skin to UV can trigger activation of the dermal blood microvasculature and alteration of the extracellular matrix, which play a key role in skin homeostasis as well as in the development of inflammatory acute processes and cutaneous neoplasia. The flavonoids present in the red grape (*Vitis vinifera*) such as quercetin, catechin, epicatechin and malvidin can protect dermal blood endothelial cells (HDBECs) *in vitro* (Di Francesco et al., 2018). In the case of MEDt, the reduction in erythema caused by UVB can be explained by the presence of sunscreen substances such as quercetin and several glycosylated derivatives such as hyperoside and avicularin (García-Bores et al., 2018) that, in addition to absorbing UV, can modulate the cellular processes that decrease the congestion of the dermal microvasculature.

3.5.2.2. Histological analysis. A histological evaluation was performed on SKH-1 hairless mice exposed to UVB. Fig. 7 shows the most representative results of the histological study. The skin of the C-group did not show histological damage (7A). Acute exposure of UVB produced histological changes in the C + UV group (7B): intra-/intercellular oedema in the epidermis (spongiosis), sunburn cells, changes in cell maturation and proliferation such as pleomorphic cells, thickening of the stratum corneum, hypertrophy and atrophy. In the dermis, vessel congestion, haemorrhage and inflammatory infiltrates were noted. Damage to the epidermis was presented in a multifocal and moderate way (7I) and increased in the dermis (7J). The MEDt group showed normal skin characteristics and some damage associated with exposure to an external agent: spongiosis, inflammatory infiltrates and congestion of blood vessels (7C). Damage was focal and slight in the epidermis (7I), with a slight increase in the dermis (7J).

By contrast, skin from MEDt UV (7D) mice showed a slight

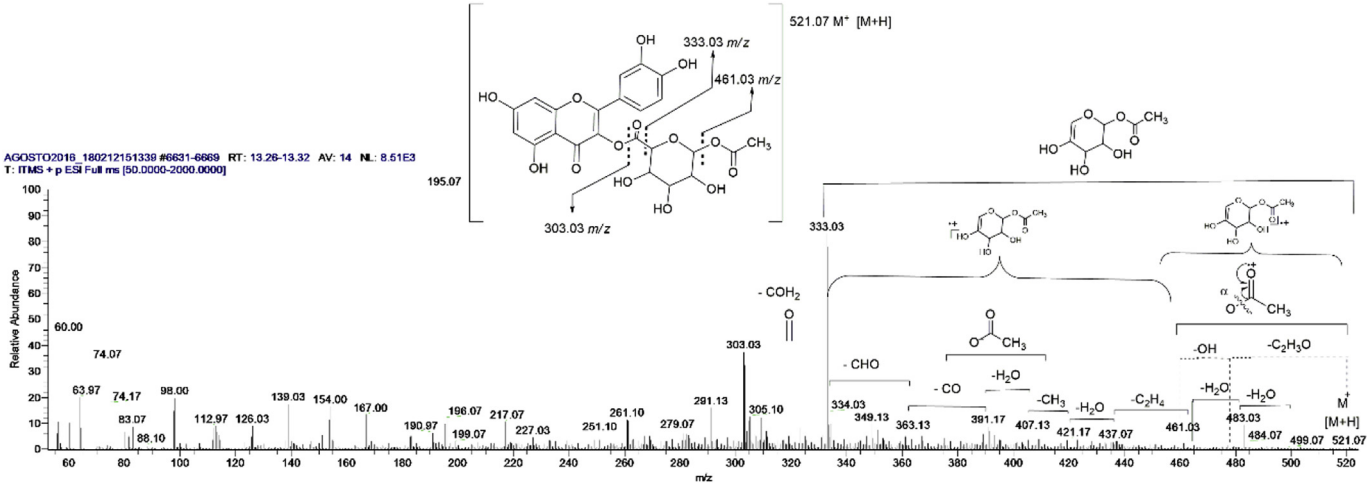

Fig. 5. Mechanism of fragmentation of proposed molecule **A3** [2-(3,4-dihydroxyphenyl)-5,7-dihydroxy-4-oxochromen-3-yl]3,4,5-trihydroxyoxane-2,6-dicarboxylate (Full mass).

Table 3
Antibacterial activity of methanolic extract *D. tagetiflora* (MEDt) obtained in different months and isolated compounds.

Organism	Inhibition halos (mm)								
	Aug 2016	Aug 2017	Sept 2017	Oct 2017	Oct 2017[a]	1	2	3	2/3 (1:4)
M. luteus	7.3 ± 0.5	na	na	na	7.7 ± 0.5	na	na	7.6 ± 0.5	9.0 ± 0.5
B. subtillis	7.0 ± 1.0	na	na	na	8.5 ± 0.9	na	na	na	na
S. marcescens	na	na	na	na	na	na	na	na	na

[a] Collected at 'Los Agustinos'. na: not activity. **1**. Hyperoside; **2**. Avicularin; **3**. Avicularin acetate. (Mean ± SD, n = 3).

Table 4
MIC and MBC of methanolic extract (MEDt) and compounds of *D. tagetiflora*.

Microorganism	Antibacterial activity (mg/mL)	MEDt October 2017[a]	Avicularin acetate	Avicularin/ Avicularin acetate (1:4)
B. subtillis	MIC	0.50	> 2.00	> 2.00
	MBC	0.75	> 2.00	> 2.00
M. luteus	MIC	0.12	1.50	> 2.00
	MBC	0.25	2.00	> 2.00

[a] Collected at 'Los Agustinos'.

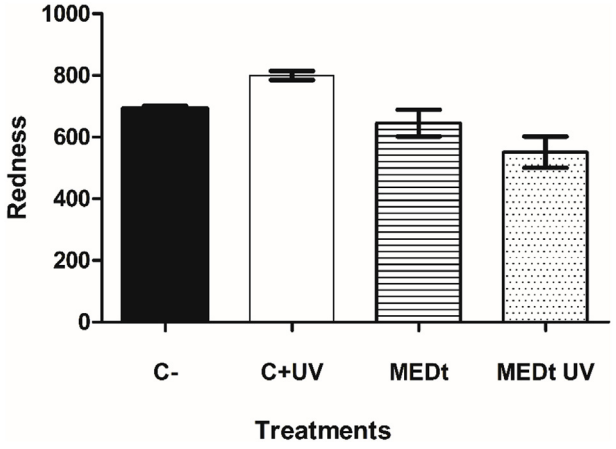

Fig. 6. Colorimetric values of erythema (redness) in SKH-1 mice. C-: Negative control (Vehicle 200 μL of ethanol); C + UV: Vehicle and UVB; MEDt: *D. tagetiflora* methanolic extract; MEDt UV: *D. tagetiflora* methanolic extract and UVB.

thickening of the epidermis and reduction of spongiosis, which were considered focal and mild (7I). The damage in the dermis included congestion of blood vessels, the presence of inflammatory infiltrates and haemorrhage, corresponding to a moderate inflammatory process (7J).

In addition to the histological diagnosis, toluidine blue staining and the mast cell count were performed (Fig. 7E–H). The results indicate that UV irradiation (7F) and the application of MEDt (7G) cause an increase in the number of mast cells in the dermis with respect to C- (7E). However, in mice treated with MEDt and subsequently exposed to UV (7H), there was a significant decrease with respect to the C + UV group, without reaching the basal levels in C- (7 E and K). This could indicate that the MEDt possibly act as an irritant on the skin. One of the most obvious characteristics of exposure to an irritant is redness. Our macroscopic results in which the skin colour was measured did not indicate that the mice of the MEDt group had a substantial increase in this parameter (Fig. 6) and in congestion at the microscopic level (Fig. 7C). Thus, more studies are needed in this regard.

Inflammation is characterized by a series of biological processes that play important roles in protecting the body against external agents, such as RUV. The steps that lead to this response are awareness and activation. In the first, the inflammatory molecules increase and inflammasomes are activated, resulting in the secretion of proinflammatory cytokines (Young-Su, 2018). Acute exposure to UV causes the recruitment of mast cells into the skin that participate in the inflammatory process characteristic of sunburn (Grimbaldeston et al., 2006). Our results confirm what was previously reported about the inflammatory effect of UV on the skin by causing damage such as the congestion of blood vessels, with the consequent haemorrhage and presence of inflammatory infiltrates (Hart et al., 2001).

The mice treated with MEDt and irradiated with UV showed a decrease in the severity of damage markers, such as thickening and oedema (spongiosis), especially in the epidermis. The combination of these two foreign agents in the skin (UV and MEDt) shows an anti-inflammatory effect in this stratum. Possibly, the chemical components of MEDt are acting as anti-inflammatory agents and modulate cellular processes. Hyperoside has anti-inflammatory properties in various models such as mouse peritoneal macrophages (Kim et al., 2011) and vascular inflammation caused by high blood glucose levels (Ku et al., 2014). Regarding avicularin, it was reported in cell cultures (SH-SY5Y and PC12) to modulate pro-inflammatory signalling (TNF-α) in neuronal cells (Park et al., 2018).

In the dermis, the extension of inflammatory markers is multifocal; however, the degree decreases that is, the severity. In addition, mast cell counts decrease significantly compared with C + UV (Fig. 7). The decrease in the number of mast cells in the dermis is an indicator of the anti-inflammatory effect of MEDt, reducing the risk of producing immunosuppression but without triggering an exacerbated inflammatory response. Mast cells in the skin participate in phototolerance or immunosuppression induced by UV so they have been directly related as a risk factor for photocarcinogenesis (Grimbaldeston et al., 2006; Schweintzger et al., 2015). UV-exposed, mast cell deficient (Kit (W-Sh/W-Sh) mice were more susceptible to epidermal hyperplasia, dermal oedema and blood vessel dilation. Thus, mast cell-deficient mice are resistant to UV-induced immune suppression and exhibit excessive scratching behaviour compared with controls. Protection from this UV-induced scratching phenotype was dependent on mast cells (Schweintzger et al., 2015).

Our results allow us to infer that the inflammatory process is modulated by the components of MEDt and that the presence of mast cells is the result of the chemoprotection mechanism of the extract, avoiding in the long term the development of skin cancer due to chronic exposure to the UV.

3.5.3. Chemoprotection in chronic experiments

The chemoprotective effects of MEDt in carcinogenesis induced by chronic exposition of UVB in mice SKH-1 are shown in Fig. 8. The appearance of skin tumours began in the 25th week of irradiation in the C + UV group, reaching 100% incidence at week 30. The multiplicity at the end of the experiment in this group was 18 (mean number of tumours/mouse). In mice treated topically with MEDt before exposure to UV-B, skin tumours arose at week 25 in 20% of the mice. At week 30, the incidence was 80% with a multiplicity of 13. Therefore, MEDt had a chemopreventive effect by reducing skin tumour development in terms of both the tumour incidence and multiplicity.

In the experiment, the number and diameters of the lesions were not constant; some disappeared or were decreased in size. It was reported

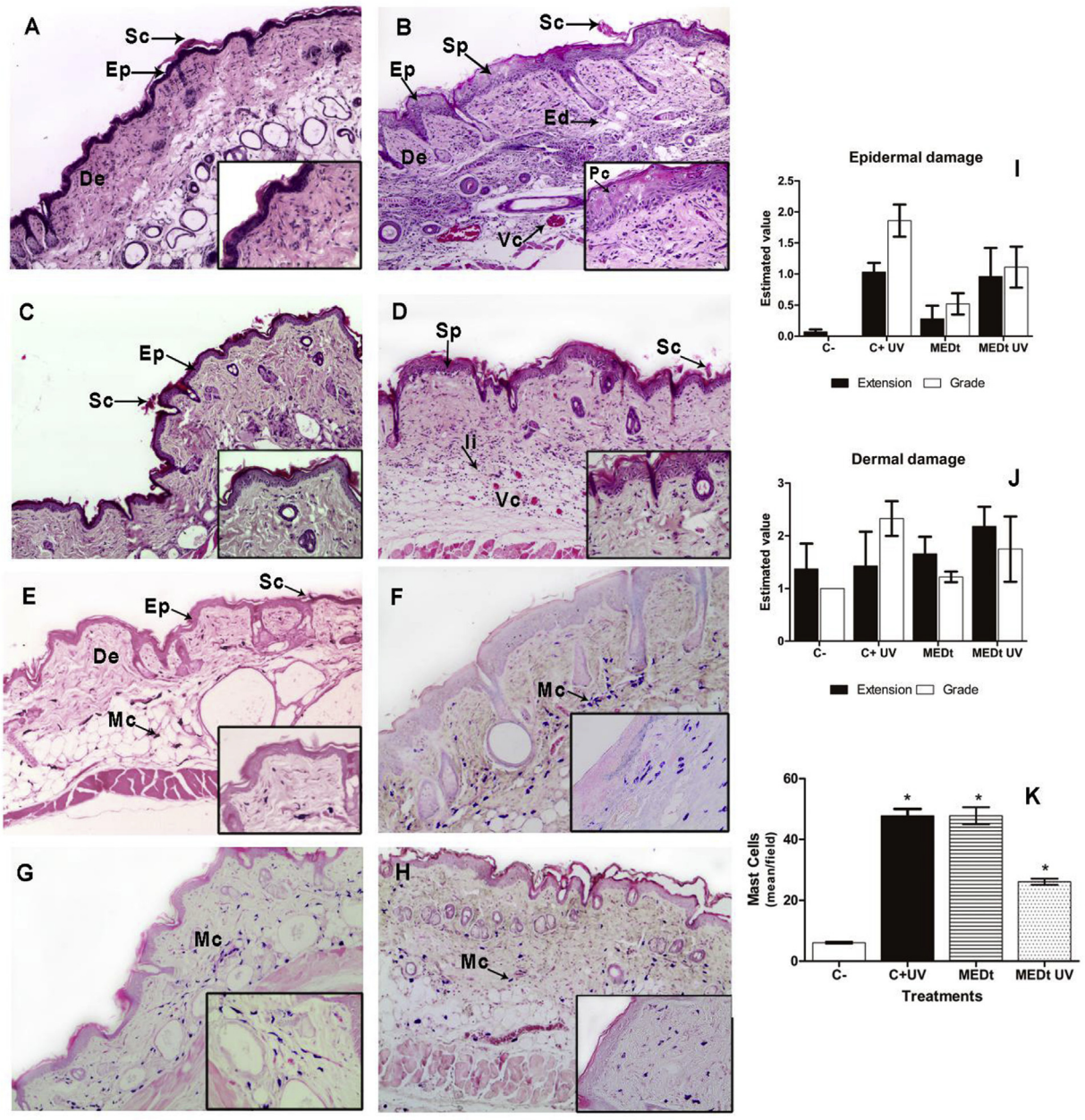

Fig. 7. Chemoprotective effect of methanolic extract of *D. tagetiflora* (MEDt). Histology of skin samples from UVB-irradiated SKH-1 mice treated with MEDt and quantitative analysis. A: C- Negative control (70% ethanol vehicle); B: C + UV (70% ethanol and UV irradiation), C: MEDt (Methanolic extract of *D. tagetiflora*); D: MEDt UV (Methanolic extract of *D. tagetiflora* and UV irradiation). Panel E–H staining for mast cell counts. E: C- Negative control; F: C + UV; G: MEDt; H: MEDt UV. Panels A–D H&E; panels E–H toluidine blue. Magnifications 100X, boxes 400X. I: Epidermal damage grouped by treatments J: Dermal damage grouped by treatments. K: Means of the number of mast cells per treatment (*$p < 0.05$ with respect to control). Ed: oedema; Ep: epidermis; De: dermis; Ii: inflammatory infiltrates; Mc: mast cell; Sc: stratum corneum; Sp: spongiosis; Pc: pleomorphic cells; Vc: vessel congestion. (For interpretation of the references to colour in this figure legend, the reader is referred to the Web version of this article.)

that injuries can heal early, which may be due to an increase in the repair of DNA damage (Roos et al., 2013). Chemoprevention is referred to preventing or delaying the development of skin cancer, particularly tumour promotion and progression stages, through using phytochemicals (Montes de Oca et al., 2017). In this case, we observed that the MEDt reduces the number of tumours in the mice, and its main components are glycosylated derivatives of quercetin. Quercetins are known to be a good antioxidant due to the hydroxyphenyl groups present in its structure. This flavonoid is an ideal candidate to prevent photocarcinogenesis; however, its poor stability, permeability and solubility diminish its potential use as a cutaneous chemoprotective agent in *in vivo* models (Hung et al., 2012). Due to the mentioned above, the activity of quercitrin (3-rhamnosyl-quercetin) has been evaluated in SKH-1 mice but only in models of semi-chronic irradiation (six weeks). Additionally, it was found to protect the skin from the generation of ROS induced by UVB and promotes the restoration of skin antioxidants such as GSH/GSSG and catalase (Yin et al., 2013). Considering the effect of quercitrin in semi-chronic experiments, the chemoprotective effect of MEDt in reducing the multiplicity of tumours induced by UVB light in SKH-1 mice can be considered to be attributed to its chemical composition in which the glycosylated derivatives of quercetin predominate.

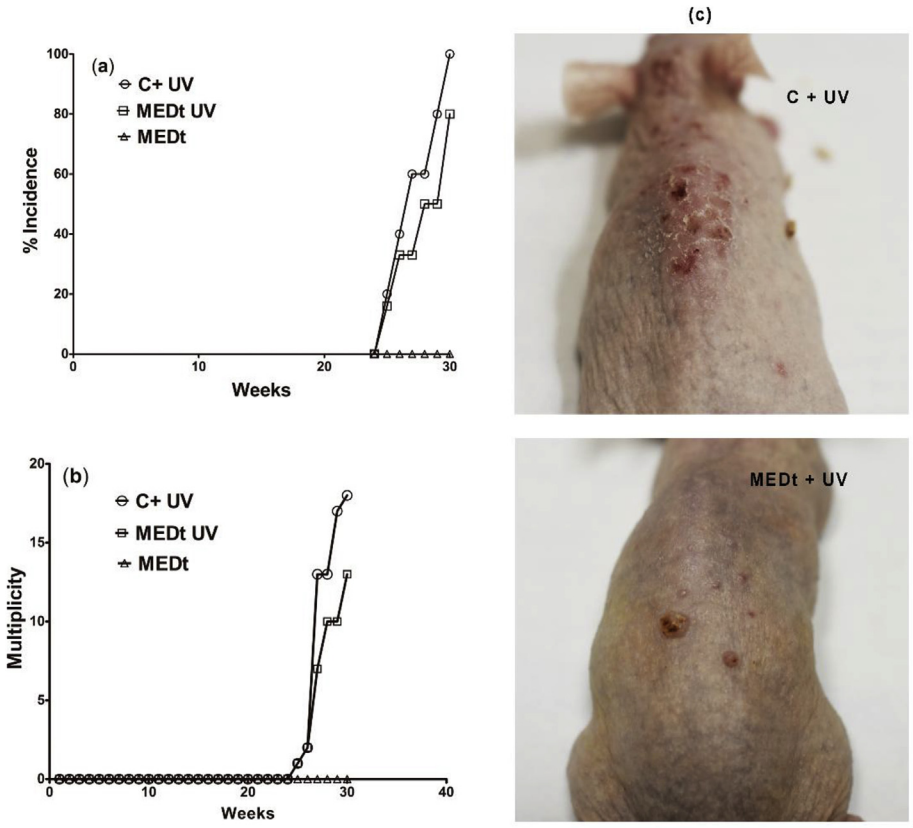

Fig. 8. Chemoprotective activity of methanolic extract of *D. tagetiflora* (MEDt) against UVB -induced skin carcinogenesis on SKH-1 mice. Multiplicity and incidence of skin tumours in mice, each point represents the mean number of tumours/mouse. C + UV: group without skin protection and chronically irradiated; MEDt UV: group with topical application of MEDt and chronically irradiated. MEDt: group with topical application of MEDt.

4. Conclusions

We reported for the first time the temporary variation of phenolic compounds in *Dyssodia tagetiflora*. Therefore, at least from August to October, *D. tagetiflora* induces similar compounds, with hyperoside being the majority compound. Additionally, we reported new compounds, not reported in *D. tagetiflora*: quercetin-4'-methyl ether 6-C glucoside, quercetin-4'-methyl ether 8-C glucoside and [2-(3,4-dihydroxyphenyl)-5,7-dihydroxy-4-oxochromen-3-yl] 3,4,5-trihydroxyoxane-2,6-dicarboxylate. Furthermore, the methanolic extract of August 2016 and October 2017 (Collected at 'Los Agustinos') presented antimicrobial activity against *M. luteus* and *B. subtillis*. Meanwhile, avicularin acetate and the mixture of avicularin/avicularin acetate presented activity only against *M. luteus*. The methanolic extract of *D. tagetiflora* has chemoprotective properties by decreasing the damage caused by acute and chronic exposure to UV in SKH-1 mice. Finally, *D. tagetiflora* is a promissory plant for subsequent research in the pursuit of novel compounds and diverse biological activity.

Conflicts of interest

The authors declare that no conflict of interest. The authors alone are responsible for the content and writing of this article.

Acknowledgements

This work was supported financially by Universidad Nacional Autónoma de México-Programa de Becas Postdoctorales (041/2017 UNAM-DGAPA), and DGAPA-PAPIIT-UNAM (Grant IN-218616). We express our gratitude to Lt. Col. Juan Pablo García Hurtado, chief Department of Pharmacology, Unit of LC-MS, Escuela Médico Militar, México. We also thank M. en C. Erick Nolasco Ontiveros, a technician at the pharmacognosy laboratory at FES-Iztacala, UNAM. We are grateful to the Department of Ecology of the Municipality of Acámbaro, Guanajuato, México for the biological material recollection facilities.

Transparency document

Transparency document related to this article can be found online at https://doi.org/10.1016/j.fct.2018.12.024.

References

Abad-García, B., Berrueta, L.A., Garmón-Lobato, Berrueta, L.A.,S., Gallo, B., Vicente, F., 2008. New features on the fragmentation and differentiation of C-glycosidic flavone isomers by positive electrospray ionization and triple quadrupole mass spectrometry. Rapid Commun. Mass Spectrom. 22, 1834–1842. https://doi.org/10.1002/rcm.3560.

Abad-García, B., Berrueta, L.A., Garmón-Lobato, S., Gallo, B., Vicente, F., 2009. A general analytical strategy for the characterization of phenolic compounds in fruit juices by high-performance liquid chromatography with diode array detection coupled to electrospray ionization and triple quadrupole mass spectrometry. J. Chromatogr. A 1216, 5398–53415. https://doi.org/10.1016/j.chroma.2009.05.039.

Avila Acevedo, J.G., Espinosa González, A.M., De Maria y Campos, D.M., Benitez Flores, J. del C., Hernández Delgado, T., Flores Maya, S., Campos Contreras, J., Muñoz López, J.L., García Bores, A.M., 2014. Photoprotection of *Buddleja cordata* extract against UVB-induced skin damage in SKH-1 hairless mice. BMC Complement Altern. Med. 3 (14), 281. https://doi.org/10.1186/1472-6882-14-281.

Bolhmann, F., Zdero, C., 1976. Inha ltsstoffe einiger gattungen der tribus Helenieae und Senecioneae. Phytochemistry 15, 1309–1310.

Bolhmann, F., Zdero, C., 1979. Über dimere terpenketone aus *Tagetes gracilis*. Phytochemistry 18, 341–343.

Cao, J., Yin, C., Qin, Y., Cheng, Z., Chen, D., 2014. Approach to the study of flavone di-C-glycosides by high performance liquid chromatography-tandem ion trap mass spectrometry and its application to characterization of flavonoid composition in *Viola yedoensis*. J. Mass Spectrom. 49, 1010–1024. https://doi.org/10.1002/jms.3413.

Cirak, C., Radusiene, J., Jakstas, V., Ivanauskas, L., Seyis, F., Yayla, F., 2017. Altitudinal changes in secondary metabolite contents of *Hypericum androsaemum* and *Hypericum polyphyllum*. Biochem. Syst. Ecol. 70, 108–115. https://doi.org/10.1016/j.bse.2016.11.006.

Conceição, L.F.R., Ferreres, F., Tavares, R.M., Dias, A.C.P., 2006. Induction of phenolic compounds in *Hypericum perforatum* L. cells by *Colletotrichum gloeosporioides* elicitation. Phytochemistry 67, 149–155. https://doi.org/10.1016/j.phytochem.2005.10.017.

Cuyckens, F., Claeys, C., 2004. Mass spectrometry in the structural analysis of flavonoids. J. Mass Spectrom. 39, 1–15. https://doi.org/10.1002/jms.585.

D'Andrea, G., 2015. Quercetin: a flavonol with multifaceted therapeutic applications?

Fitoterapia 106, 256–271. https://doi.org/10.1016/j.fitote.2015.09.018.
Davis, B.D., Brodbelt, J.S., 2004. Determination of the glycosylation site of flavonoid monoglucosides by metal complexation and tandem mass spectrometry. J. Am. Soc. Mass Spectrom. 15, 287–299 0.1016/j.jasms.2004.06.003.
De Villiers, A., Venter, P., Pasch, H., 2016. Recent advances and trends in the liquid-chromatography–mass spectrometry analysis of flavonoids. J. Chromatogr. A 1430, 16–78. https://doi.org/10.1016/j.chroma.2015.11.077.
Di Francesco, S., Savio, M., Bloise, N., Borroni, G., Stivala, L.A., Borroni, R.G., 2018. Red grape (*Vitis vinifera* L.) flavonoids down-regulate collagen type III expression after UV-A in primary human dermal blood endothelial cells. Exp. Dermatol. https://doi.org/10.1111/exd.13682.
Downum, K.R., Towers, H.N., 1983. Analysis of thiophenes in the *Tageteae* (Astaraceae) by HPLC. J. Nat. Prod. 46, 98–103. https://doi.org/10.1021/np50025a008.
Downum, K.R., Keil, D.J., Rodríguez, E., 1985. Distribution of acetiylenic thiophenes in Pectidinae. Biochem. Syst. Ecol. 13, 109–113.
Elder, D., Elenistas, R., Jaworsky, C., Johnson, B., 1997. In: Lever's Histopatology of the Skin, eighth ed. Lippincott-Raven, USA.
Espinosa González, A.M., García Bores, A.M., Benítez Flores, J.C., Sandoval Pérez, C.E., González Valle, M.R., Céspedes, P.C.L., Avila Acevedo, J.G., 2016. Photoprotective effect of verbascoside from *Buddleja cordata* in mice SKH-1 exposed to acute and chronic UVB radiation. Bol. Latinoam. Caribe Plantas Med. Aromat. (BLACPMA) 15, 288–300. https://doi.org/10.1186/1472-6882-14-281.
Faizi, S., Ali, M., 1999. Shamimin: a new flavonol C-glycoside from leaves of *Bombax ceiba*. Planta Medica 65 (4), 383–385. https://doi.org/10.1055/s-2006-960796.
Ferreres, F., Silva, B.M., Andrade, P.B., Seabra, R.M., Ferreira, M.A., 2003. Approach to the study of C-glycosyl flavones by ion trap HPLC-PAD-ESI/MS/MS: application to seeds of quince (*Cydonia oblonga*). Phytochem. Anal. 14, 352–359. https://doi.org/10.1002/pca.727.
Gallagher, C.H., Canfield, P.J., Greenoak, G.E., Reeve, V.E., 1984. Characterization and histogenesis of tumors in the hairless mouse produced by low-dosage incremental ultraviolet radiation. J. Invest. Dermatol. 83 (3), 169–174. https://doi.org/10.1111/1523-1747.ep12263512.
García-Bores, A.M., Arciniegas-Arciniegas, A., Reyna-Campos, A., Céspedes-Acuña, C., Avila-Suárez, B., Alarcón-Enos, J., Flores-Maya, S., Espinosa-González, A.M., de Vivar-Romo, A.R., Pérez-Plasencia, C., Avila-Acevedo, J.G., 2018. Phytochemical composition and biological activities of *Dyssodia tagetiflora* Lag. Chem. Biodivers. 15. https://doi.org/10.1002/cbdv.201700415.
Geng, P., Sun, J., Zhang, M., Li, X., Harnly, J.M., Chen, P., 2016. Comprehensive characterization of C-glycosyl flavones in wheat (*Triticum aestivum* L.) germ using UPLC-PDA-ESI/HRMS and mass defect filtering. J. Mass Spectrom. 51, 914–930. https://doi.org/10.1002/jms.3803.
Grayer, R.J., Kite, G.C., Abou-Zaid, M., Archer, L.J., 2000. The application of atmospheric pressure chemical ionization liquid chromatography-mass spectrometry in the chemotaxonomic study of flavonoids: characterization of flavonoids from *Ocimum gratissimum* var. gratissimum. Phytochem. Analysis. 11, 257–267. https://doi.org/10.1002/1099-1565(200007/08)11:4<257::AID-PCA521>3.0.CO;2-A.
Grimbaldeston, M.A., Finlay-Jones, J.J., Hart, P.H., 2006. Mast cells in photodamaged skin: what is their role in skin cancer? Photochem. Photobiol. Sci. 5, 177–183. https://doi.org/10.1039/b504344a.
Harborne, J.B., 1994. The Flavonoids Advances in Research since 1986. Chapman & Hall, New York, NY.
Hart, P.H., Grimbaldeston, M.A., Finlay-Jones, J.J., 2001. Sunlight, immunosuppression and skin cancer: role of histamine and mast cells. Clin. Exp. Pharmacol. Physiol. 28, 1–8. https://doi.org/10.1046/j.1440-1681.2001.03392.x.
Hatahet, T., Morille, M., Hommoss, A., Devoisselle, J.M., Müller, R.H., Bégu, S., 2016. Quercetin topical application, from conventional dosage forms to nanodosage forms. Eur. J. Pharm. Biopharm. 108, 41–53. https://doi.org/10.1016/j.ejpb.2016.08.011.
Hung, C.-F., Fang, C.-L., Al-Suwayeh, S.A., Yang, S.-Y., Fang, J.-Y., 2012. Evaluation of drug and sunscreen permeation via skin irradiated with UVA and UVB: comparisons of normal skin and chronologically aged skin. J. Dermatol. Sci. 68, 135–148. https://doi.org/10.1016/j.jdermsci.2012.09.005.
Kim, S.J., Um, J.Y., Lee, J.Y., 2011. Anti-inflammatory activity of hyperoside through the suppression of nuclear factor-κB activation in mouse peritoneal macrophages. Am. J. Chin. Med. 39, 171–181. https://doi.org/10.1142/S0192415X11008737.
Koneman, E.W., Procop, G.W., Church, D.L., Hall, G.S., Janda, W.M., Schreckenberger, P.C., Woods, G.L., 2017. In: Diagnóstico Microbiológico, seventh ed. LWW. España.
Ku, S.K., Kwak, S., Kwon, O.J., Bae, J.S., 2014. Hyperoside inhibits high-glucose-induced vascular inflammation *in vitro* and *in vivo*. Inflammation 37, 1389–1400. https://doi.org/10.1007/s10753-014-9863-8.
Lademann, J., Jacobi, U., Surber, C., Weigmann, H.J., Fluhr, J.W., 2009. The tape stripping procedure–evaluation of some critical parameters. Eur. J. Pharm. Biopharm. 72, 317–323. https://doi.org/10.1016/j.ejpb.2008.08.008.
Lashmar, U.T., Hadgraft, J., Norman, T., 1988. Topical application of penetration enhancers to the skin of nude mice: a histopatological study. J. Pharm. Pharmacol. 41, 118–121. https://doi.org/10.1111/j.2042-7158.1989.tb06405.x.
Marín-Loaiza, J.C., Avila, J.G., Canales, M., Hernández, T., Céspedes, C.L., 2008. Antifungal and antibacterial activities of *pittocaulon* spp. Pharm. Biol. 46, 66–71. https://doi.org/10.1080/13880200701734505.
Marotti, I., Marotti, M., Piccaglia, R., Nastri, A., Grandi, S., Dinelli, G., 2010. Thiophene occurrence in different *Tagetes* species: agricultural biomasses as source of biocidal substances. J. Sci. Food Agric. 90, 1210–1217. https://doi.org/10.1002/jsfa.3950.
Materska, M., 2008. Quercetin and its derivatives: chemical structure and bioactivity - a review. Pol. J. Food Nutr. Sci. 58, 407–413.
Montes de Oca, M.K., Pearlman, R.L., McClees, S.F., Strickland, R., Afaq, F., 2017. Phytochemicals for the prevention of photocarcinogenesis. Photochem. Photobiol. 93, 956–974. https://doi.org/10.1111/php.12711.
Nurmi, K., Ossipov, V., Haukioja, E., Pihlaja, K., 1996. Variation of total phenolic content and individual low-molecular-weight phenolics in foliage of mountain birch trees (*Betula pubescens* ssp. tortuosa). J. Chem. Ecol. 22, 2023–2040. https://doi.org/10.1007/BF02040093.
Park, S.H., Jang, S., Son, E., Lee, S.W., Park, S.D., Sung, Y.Y., Kim, H.K., 2018. *Polygonum aviculare* L. extract reduces fatigue by inhibiting neuroinflammation in restraint-stressed mice. Phytomedicine 42, 180–189. https://doi.org/10.1016/j.phymed.2018.03.042.
Pereira, C.A., Yariwake, J.H., McCullagh, M., 2005. Distinction of the C-glycosylflavone isomer pairs orientin/isoorientin and vitexin/isovitexin using HPLC-MS exact mass measurement and in-source CID. Phytochem. Anal. 16, 295–301. https://doi.org/10.1002/pca.820.
Pikulski, M., Brodbelt, J.S., 2003. Differentiation of flavonoid glycoside isomers by using metal complexation and electrospray ionization mass spectrometry. J. Am. Soc. Mass Spectrom. 14, 1437–1453. https://doi.org/10.1016/j.jasms.2003.07.002.
Robbins, S.L., Cotran, R.S., Kumar, V.M.D., 2008. In: Patología Estructural Y Funcional, eighth ed. Elsevier, España.
Rojas, A., Bah, M., Rojas, J.I., Serrano, V., Pacheco, P., 1999. Spasmolytic activity of some plants used by the Otomi Indians of Querétaro (México) for the treatment of gastrointestinal disorders. Phytomedicine 6, 367–371. https://doi.org/10.1016/S0944-7113(99)80061-0.
Roos, W.P., Kaina, B., 2013. DNA damage-induced cell death: from specific DNA lesions to the DNA damage response and apoptosis. Cancer Lett. 237–248. https://doi.org/10.1016/j.canlet.2012.01.007.
Sánchez-Blanco, J., Guevara-Féfer, F., 2013. Plantas arvenses asociadas a cultivos de maíz de temporal en suelos salinos de la Ribera del lago de Cuitzeo, Michoacán, México. Acta Bot. Mex. 105, 107–129.
Sánchez-Rabaneda, F., Jáuregui, O., Casals, I., Andrés-Lacueva, C., Izquierdo-Pulido, M., Lamuela-Raventós, R.M., 2003. Liquid chromatographic/electrospray ionization tandem mass spectrometric study of the phenolic composition of cocoa (*Theobroma cacao*). J. Mass Spectrom. 38, 35–42. https://doi.org/10.1002/jms.395.
Schweintzger, N.A., Bambach, I., Reginato, E., Mayer, G., Limón-Flores, A.Y., Ullrich, S.E., Byrne, S.N., Wolf, P., 2015. Mast cells are required for phototolerance induction and scratching abatement. Exp. Dermatol. 24, 491–496. https://doi.org/10.1111/exd.12687.
Sharma, M.R., Werth, B., Werth, V.P., 2011. Animal models of acute photodamage: comparisons of anatomic, cellular and molecular responses in C57BL/6J, SKH1 and Balb/c mice. Photochem. Photobiol. 87, 690–698. https://doi.org/10.1111/j.1751-1097.2011.00911.x.
Sharma, A., Kashyap, D., Sak, K., Tuli, H.S., Sharma, A.K., 2018. Therapeutic charm of quercetin and its derivatives: a review of research and patents. Pharm Pat Anal 7, 15–32. https://doi.org/10.4155/ppa-2017-0030.
Simkhada, D., Kurumbang, N., Lee, H.C., Sohng, J.K., 2010. Exploration of glycosylated flavonoids from metabolically engineered *E. coli*. Biotechnol. Bioprocess Eng. 15, 754–760. https://doi.org/10.1007/s12257-010-0012-4.
Singh, A., Kumar, S., Bajpai, V., Reddy, T.J., Rameshkumar, K.B., Kumar, B., 2015. Structural characterization of flavonoid C- and O-glycosides in an extract of *Adhatoda vasica* leaves by liquid chromatography with quadrupole time-of-flight mass spectrometry. Rapid Commun. Mass Spectrom. 29, 1095–1106. https://doi.org/10.1002/rcm.7202.
Tellez, M.R., Estell, R.E., Fredrickson, L., Havstad, K.M., 1997. Essential oil of *Dyssodia acerosa* DC. J. Agric. Food Chem. 45, 3276–3278. https://doi.org/10.1021/jf9701502.
Trujillo, O., Vanezis, P., Cermignanib, M., 1996. Photometric assessment of skin colour and lightness using a tristimulus calorimeter: reliability of inter and intra-investigator observations in healthy adult volunteers. Forensic Sci. Int. 81, 1–10.
Villareal-Quintanilla, J.A., Villaseñor-Ríos, J.L., Medina-Lemos, R., 2008. In: Flora del Valle de Tehuacán: familia Astareaceae, tribu Tageteae 62. Universidad Nacional Autónoma de México, fascículo, pp. 1–59.
Wang, Z.Y., Huang, M.T., Ferraro, T., Wong, C.Q., Lou, Y.R., Reuhl, K., Iatropoulos, M., Yang, C.S., Conney, A.,H., 1992. Inhibitory effect of green tea in the drinking water on tumorigenesis by ultraviolet light and 12-0-tetradecanoylphorbol-13-acetate in the skin of SKH-1 mice. Cancer Res. 52, 1162–1170. https://doi.org/10.1016/0091-7435(92)90043-H.
Waridel, P., Wolfender, J.L., Ndjoko, K., Hobby, K.R., Major, H.J., Hostettmann, K., 2001. Evaluation of quadrupole time-of-flight tandem mass spectrometry and ion-trap multiple-stage mass spectrometry for the differentiation of C-glycosidic flavonoid isomers. J. Chromatogr. A 926, 29–41. https://doi.org/10.1016/S0021-9673(01)00806-8.
Wissing, S.A., Müller, R.H., 2002. Solid lipid nanoparticles as Carrier for sunscreens: *in vitro* release and *in vivo* skin penetration. J. Contr. Release 81, 225–233. https://doi.org/10.1016/S0168-3659(02)00056-1.
Wu, T., He, M., Zang, X., Zhou, Y., Qiu, T., Pan, S., Xu, X., 2013. A structure–activity relationship study of flavonoids as inhibitors of *E. coli* by membrane interaction effect. Biochim. Biophys. Acta 1828, 2751–2756. https://doi.org/10.1016/j.bbamem.2013.07.029.
Xiao, J., Capanoglu, E., Jassbi, A.R., Miron, A., 2016. Advance on the flavonoid C-glycosides and health benefits. Crit. Rev. Food Sci. Nutr. 29, 29–45. https://doi.org/10.1080/10408398.2015.1067595.
Yin, Y., Li, W., Son, Y.O., Sun, L., Lu, J., Kim, D., Wang, X., Yao, H., Wang, L., Pratheeshkumar, P., Hitron, A.J., Luo, J., Gao, N., Shi, X., Zhang, Z., 2013. Quercitrin protects skin from UVB-induced oxidative damage. Toxicol. Appl. Pharmacol. 269, 89–99. https://doi.org/10.1016/j.taap.2013.03.015.
Young-Su, Y., 2018. Regulatory roles of flavonoids on inflammasome activation during inflammatory responses. Mol. Nutr. Food Res. 1. https://doi.org/10.1002/mnfr.201800147.